

# Magnetic ground state of coupled edge-sharing CuO<sub>2</sub> spin-chains

U. Schwingenschlögl and C. Schuster

*Institut für Physik, Universität Augsburg, 86135 Augsburg, Germany*

(Dated: November 23, 2018)

By means of density functional theory, we investigate the magnetic ground state of edge-sharing CuO<sub>2</sub> spin-chains, as found in the (La,Ca,Sr)<sub>14</sub>Cu<sub>24</sub>O<sub>41</sub> system, for instance. Our data rely on spin-polarized electronic structure calculations including onsite interaction (LDA+U) and an effective model for the interchain coupling. Strong doping dependence of the magnetic order is characteristic for edge-sharing CuO<sub>2</sub> spin-chains. We determine the ground state magnetic structure as function of the spin-chain filling and quantify the competing exchange interactions.

PACS numbers: 71.10.Pm, 71.20.-b, 75.25.+z, 75.30.Et

Keywords: density functional theory, electronic structure, magnetic chain

Doping of magnetic systems nowadays attracts great interest due to a large number of exotic effects. 3D antiferromagnetic order, for example, is easily destroyed by either quantum or thermodynamical fluctuations, and by any kind of impurity. The study of doped 2D antiferromagnets [1] has been triggered by the phase diagrams of high-temperature superconductors. Upon doping, they show a transition from an antiferromagnetic to a superconducting state. On the other hand, 1D copper oxide compounds are an active field of research, too. From the theoretical point of view, the magnetic properties of undoped two-leg Cu<sub>2</sub>O<sub>3</sub> ladders are explained in terms of a Heisenberg model with cyclic ring exchange [2]. Doping effects are investigated in Refs. [3, 4]. Antiferromagnetic CuO chains with 180° Cu-O-Cu bond angles, as found in Sr<sub>2</sub>CuO<sub>3</sub> [5], for example, can be understood by conformal field theory [6]. When a few Cu ions are replaced by non-magnetic ions, like Zn, the system is well described by the Heisenberg model with removed spins [7]. Edge-sharing CuO<sub>2</sub> chains with 90° Cu-O-Cu bond angles, on the contrary, are frustrated due to competition between ferromagnetic and antiferromagnetic exchange [8, 9, 10]. In this context, both charge and spin order of highly doped systems are not understood by far.

The (Sr,Ca,La)<sub>14</sub>Cu<sub>24</sub>O<sub>41</sub> system of isostructural materials is prototypical for doping dependent charge and magnetic ordering in a partially filled spin-chain, i.e. a chain with less than one spin per site. The compounds have been subject of intensive research in recent years, mainly due to a rich phase diagram and a close relation to cuprate superconductors. The incommensurate crystal structures consist of planes of quasi 1D CuO<sub>2</sub> chains running along the crystallographic *c*-axis, stacked alternately with planes of two-leg Cu<sub>2</sub>O<sub>3</sub> ladders. The lattice constants of these subsystems satisfy  $10c_{\text{chain}} \approx 7c_{\text{ladder}}$  [11, 12]. Materials with different Sr/Ca composition are isostructural with only minor modifications of the bond lengths and angles [13, 14, 15]. A relative shift between adjacent chains parallel to the chain axis distinguishes Sr and Ca rich compounds. In Ca<sub>13.6</sub>Sr<sub>0.4</sub>Cu<sub>24</sub>O<sub>41</sub> the shift amounts to half the intrachain Cu-Cu distance, while it is only 30% of this distance for Sr<sub>14</sub>Cu<sub>24</sub>O<sub>41</sub>. For each Sr/Ca composition the Cu valence is 2.25, where Cu<sup>2+</sup>

ions ( $S = 1/2$ ) accumulate on the ladders. In contrast, most of the 6 Cu<sup>3+</sup> ions per unit cell, which form  $S = 0$  Zhang-Rice singlets (so-called holes), are located on the chains. Optical conductivity and x-ray absorption data suggest that substitution of Ca for Sr induces a transfer of holes back into the ladders [16, 17]. Consequently, an average Cu valence of 2.50 is assumed for the chain sites in Ca rich samples, giving rise to a half filled chain with one spin per two sites. On La substitution the intrinsic doping decreases gradually, reaching the undoped state with a nominal Cu valence of 2.00 for La<sub>6</sub>Ca<sub>8</sub>Cu<sub>24</sub>O<sub>41</sub>.

By chain geometry, competing ferromagnetic nearest-neighbour and antiferromagnetic next-nearest neighbour coupling is expected for edge-sharing CuO<sub>2</sub> spin-chains. The magnetic phase diagram comprises at least 3 phases upon doping, i.e. variation of the number of holes in the spin-chain. In the case of Sr<sub>14</sub>Cu<sub>24</sub>O<sub>41</sub> the CuO<sub>2</sub> chains are non-magnetic with a spin gap of about 130 K, which can be explained in a dimer picture [18]. Using a cluster calculation, Gelleé and Lepetit [19] have shown that the ground state is very complex, with trimer contributions. A dimer ground state is found by exact diagonalization of a Heisenberg model with nearest and next-nearest neighbour interaction [20], in accordance with band structure data [21]. On the contrary, antiferromagnetic intrachain ordering has been reported for Ca rich samples [15, 22]. Despite a huge number of investigations, most details of the antiferromagnetic order are still a matter of controversy. Even worse, in Sr<sub>13</sub>LaCu<sub>24</sub>O<sub>41</sub> spin dimers evolve instead of the antiferromagnetism expected for half filled chains [23]. Reflecting Cu-O-Cu bond angles of  $\approx 90^\circ$ , ferromagnetism finally is realized in slightly doped spin-chains of La rich systems [24, 25], which are captured by a 2D classical Heisenberg model with defects [26].

Spin-chain systems are strongly affected by both subtleties of the crystal structure and the electron-electron interaction. In the case of half filled spin-chains [27] the ground state magnetic structure has been established in [28]. However, the dependence of the exchange coupling on the filling  $n$  (where  $n = \text{number of spins} / \text{number of sites}$ ) is an open question, since the coupling over a hole competes with the coupling over an interstitial spin. In order to obtain a comprehensive picture of doped spin-

<b>staggered</b>	fm	afm	$4k_F$ /afm	cluster
$U = 0$ Ryd: $E - E_0$ (mRyd)	45	—	15	0.3
$U = 0.3$ Ryd: $E - E_0$ (mRyd)	19	21	27	—

<b>symmetric</b>	fm	afm	$4k_F$ /afm	cluster
$U = 0$ Ryd: $E - E_0$ (mRyd)	-6	—	64	1
$U = 0.3$ Ryd: $E - E_0$ (mRyd)	18	27	66	—

TABLE I: Total energy gain (per Cu atom) with respect to a non-magnetic calculation, for both staggered and symmetrically aligned spin-chains. The fm, afm,  $4k_F$ /afm, and cluster spin patterns are compared to each other [28]. The filling of the spin-chain is  $n = 1/2$ .

chains, we thus clarify the details of the transition from antiferromagnetic to ferromagnetic coupling on reducing the hole count. To be more specific, we study the onset of ferromagnetism at  $n = 2/3$  and the full spin chain at  $n = 1$  for typical Cu-Cu bond lengths of  $2.75 \text{ \AA}$  (nearest neighbour) and  $5.8 \text{ \AA}$  (next-nearest neighbour).

The following results are based on density functional theory and the generalized gradient approximation. We apply the WIEN2k program package, a state-of-the-art full-potential code with a mixed lapw and apw+lo basis [29]. For all the spin configurations under investigation, the charge density is represented by at least 70,000 plane waves and the Brillouin zone integration uses a  $\mathbf{k}$ -mesh comprising at least 18  $\mathbf{k}$ -points in the irreducible wedge. While Cu  $3p$  and O  $2s$  orbitals are treated as semi-core states, the valence states contain Cu  $3d$ ,  $4s$ ,  $4p$  and O  $2p$ ,  $3s$  orbitals. To achieve a mixed valence in a unit cell with both  $\text{Cu}^{3+}$  and  $\text{Cu}^{2+}$  ions, we start the calculation from the following setup: One electron is added to each oxygen, thus preventing charge transfer off the copper, and restricted to a Watson sphere of radius  $1.3 \text{ \AA}$ . Moreover, a  $3d^{10}$  configuration is used for the  $\text{Cu}^{3+}$  ions and a  $3d^{10}4s^1$  configuration for the  $\text{Cu}^{2+}$  ions.

From a structural point of view, the spin-chain materials  $(\text{La,Ca,Sr})_{14}\text{Cu}_{24}\text{O}_{41}$  consist of 3 subsystems: The

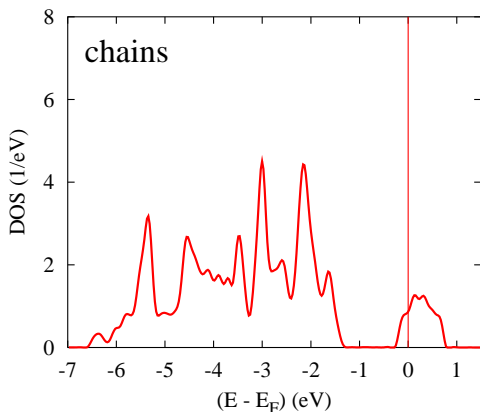


FIG. 1: Density of states (DOS) for the chain subsystem of  $\text{Sr}_{14}\text{Cu}_{24}\text{O}_{41}$ . [33]

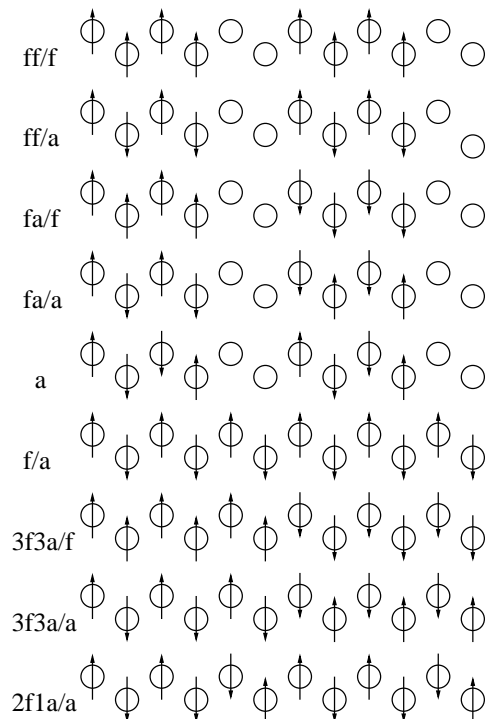


FIG. 2: Nomenclature of spin patterns on coupled chains.

$\text{CuO}_2$  spin-chains,  $\text{Cu}_2\text{O}_3$  ladders, and interstitial electron donor ions. As interaction between the subsystems is very small, an effective model of coupled spin-chains, capturing structural prerequisites of the exchange interaction, may be used to investigate the compounds [21]. The density of states (DOS) of the  $\text{CuO}_2$  chains shows a structure of width  $\approx 5.2 \text{ eV}$  at binding energies larger than  $2 \text{ eV}$  and a second structure of width  $1 \text{ eV}$  right at the Fermi level. As expected for transition metal oxides [30, 31, 32], the states are due to bonding between Cu  $3d_{xz}$  and O  $2p_x/p_z$  orbitals. Characteristic Cu  $3d_{xz}$  bands at the Fermi energy dominate the electronic and magnetic properties [33]. A tight-binding fit reveals strong next-nearest neighbour hopping, which is rather independent of the interchain coupling. Nearest neighbour hopping, in contrast, can be suppressed by relative shifts between the  $\text{CuO}_2$  chains. In that case the transverse hopping, a measure of the 2D coupling, increases [21].

For  $n = 1/2$ , the local density approximation (LDA), not accounting for the onsite interaction, yields a ferromagnetic ground state for staggered spin-chains [28]. In contrast, antiferromagnetic spin order and  $4k_F$ -periodic charge order, complemented by antiferromagnetic interchain coupling, are observed for symmetric spin-chains, compare the data in Table I. In this case, the ferromagnetic solution is even unstable. Including local electron-electron interaction at the correlated Cu  $3d$  orbitals, an LDA+U treatment reveals an antiferromagnetic ground state in both arrangements, see Table I. A relative shift between the  $\text{CuO}_2$  chains promotes antiferromagnetism

	ff/f	ff/a→f/a	fa/f→3f3a/f	fa/a→3f3a/a	a
U = 0 Ryd: E - E <sub>0</sub> (mRyd)	5	12	3	5	9
	ff/f	f/a	3f3a/f	3f3a/a	a→2f1a/a
U = 0.3 Ryd: E - E <sub>0</sub> (mRyd)	27	32	30	30	28

TABLE II: Total energy gain (per Cu atom) with respect to a non-magnetic calculation for the spin-chain filling factor  $n = 2/3$ . Several spin patterns are compared to each other, see fig. 2 for the nomenclature.

	f/f	f/a	a
U = 0 Ryd: E - E <sub>0</sub> (mRyd)	-16	45	105
U = 0.3 Ryd: E - E <sub>0</sub> (mRyd)	30	28	30

TABLE III: Total energy gain (per Cu atom) with respect to a non-magnetic calculation for a full spin-chain ( $n = 1$ ). The f/f, f/a, and a spin patterns are compared to each other.

more effectively than a local interaction. In total, next-nearest neighbour coupling over a hole site controls the magnetism in a half filled spin-chain. The combination of electron-electron repulsion and structural frustration therefore gives rise to a  $4k_F$  spin pattern. Due to a weak interchain coupling of about 1 mRyd, the magnetic next-nearest neighbour interaction energy is  $54 \pm 2$  mRyd per Cu atom within the chain.

Turning to a lower hole doping, we start with the filling  $n = 2/3$  and afterwards consider the full spin-chain, given by  $n = 1$ . For  $n = 2/3$ , we have 4 Cu<sup>2+</sup> ions per 6 lattice sites on the coupled chains. The supercell entering the band structure calculation therefore contains 12 inequivalent Cu sites. We set up the start configuration as follows: Within a chain, a ferro- or antiferromagnetic two spin cluster is coupled to the next such cluster over a hole site. Experimental data rather point at antiferromagnetic than ferromagnetic coupling between adjacent chains [25]. However, as the details of the exchange interaction are not known, we study both possibilities for comparison. This leads to altogether five configurations, which we systematically call ff/f, fa/f, ff/a, fa/a and a. For clarity, these configurations are depicted in fig. 2. In each case, we calculate the total energy and compare it to the findings of a spin-degenerate calculation, yielding the energy gain due to the exchange interaction.

The fully ferro- (ff/f) and antiferromagnetic (a) cluster spin configurations in the following serve as a reference frame for the discussion. Without local electron-electron interaction, only these two patterns are found to be stable. The magnetic moments are  $\approx 0.35\mu_B$  on the Cu<sup>2+</sup>-sites, where moments connected to two holes are slightly larger than those connected to a single hole. Ferromagnetic clusters with antiferromagnetic intrachain coupling (fa/f and fa/a) transform into modified clusters without intermediate holes, therefore into a more homogeneous charge distribution. According to the initial interaction, we obtain a 3f3a/f or 3f3a/a spin pattern, as depicted in fig. 2. Ferromagnetic intrachain coupling in combination

with antiferromagnetic interchain coupling (ff/a) results in a homogeneous spin-chain (fa). For the spin patterns under consideration, table II compares the total energy gain due to the magnetic exchange interaction.

When we account for a local electron-electron interaction  $U = 0.3$  Ryd by means of the LDA+U method, the spin patterns ff/f, 3f3a/f, 3f3a/a and f/a remain stable, where the magnetic moments increase slightly to about  $0.5\mu_B$ . Only the fully antiferromagnetic cluster configuration develops a more homogeneous charge distribution given by the spin pattern 2f1a/a, as shown in fig. 2. We obtain the largest total energy gain (with respect to the non-magnetic state) for the f/a spin pattern, amounting to 32 mRyd per Cu site. The magnetic ground state of edge-sharing CuO<sub>2</sub> chains with filling  $n = 2/3$  therefore is given by fully polarized ferromagnetic spin-chains and antiferromagnetic interchain coupling. Remarkably, the electronic correlations do not alter the magnetic ground state, see the  $U = 0$  Ryd data in table II. As compared to the coupling in a half filled spin-chain, ferromagnetic nearest neighbour interaction here becomes dominant as the electron-electron repulsion supports a homogeneous charge distribution. Whereas we find the onset of ferromagnetism already for  $n = 2/3$ , experiments on La-rich systems suggest a nominal filling of about  $n = 0.7$ . We ascribe this discrepancy to insufficient knowledge about the effective chain hole count in the real materials. By the data given in table II, we conclude that the energy gain due to the interchain magnetic coupling is at most 1 mRyd per lattice site. In addition, comparison of the f/a to the 2f1a/a data allows us to estimate an energy difference of 1.3 mRyd between the ferro- and antiferromagnetic coupling of neighbouring spins. The combination of the ff/f data with the half filled spin chain results in an intrachain nearest neighbour exchange interaction energy of  $27 \pm 2$  mRyd per Cu atom. Therefore, the next-nearest neighbour coupling is found to be almost exactly twice as strong as the nearest neighbour coupling.

For the full spin-chain ( $n = 1$ ), we address ferro- and antiferromagnetically coupled CuO<sub>2</sub> chains with a ferromagnetic intrachain coupling (f/f and f/a), and a frustrated antiferromagnet (a). For all three configurations the band structure calculation converges with magnetic moments of about  $0.4\mu_B$ . The antiferromagnet has the lowest energy, both for  $U = 0$  Ryd and a moderate local electron-electron interaction (of  $U = 0.3$  Ryd), see table III. In the latter case, the magnetic moments increase to  $0.6\mu_B$  for the antiferromagnet. In contrast to the doped

compounds, a local interaction now counteracts the spin ordering. By an energy difference of less than 0.2 mRyd per lattice site, ferro- and antiferromagnetic interaction between nearest neighbour spins result in almost degenerate electronic states. On the contrary, the energy gain due to the interchain coupling is larger than determined for the spin-chain fillings  $n = 1/2$  and  $n = 2/3$ .

In conclusion, we have investigated the magnetic coupling in edge-sharing  $\text{CuO}_2$  chains with  $\approx 90^\circ$  Cu-O-Cu bond angles, at doping levels of  $n = 1/2$ ,  $n = 2/3$ , and  $n = 1$ . By means of LDA+U electronic structure calculations, we have studied the total energy for various spin patterns. Our data shows that accounting for both the chain geometry and the electron-electron interaction [34] is essential for obtaining a comprehensive picture of the magnetism, though electronic correlation does not alter the magnetic ground state. For symmetric  $\text{CuO}_2$  chains and filling  $n = 1/2$  the latter is antiferromagnetic with a  $4k_F$  charge order along the chain axis. Adjacent chains are coupled antiferromagnetically, too. This result particularly applies to the coupled  $\text{CuO}_2$  chains of Ca-rich spin-chain materials  $(\text{Sr,Ca})_{14}\text{Cu}_{24}\text{O}_{41}$ . La-rich systems

with spin-chain filling  $n = 2/3$  develop a ferromagnetic intrachain coupling since Coulomb repulsion supports a homogeneous distribution of the charge. The interchain coupling remains antiferromagnetic. When the filling is complete ( $n = 1$ ), finally a frustrated antiferromagnet is found, which fact reflects strong electronic correlations. Under the assumption that modelling in terms of a Hubbard model is appropriate, antiferromagnetism supports intrachain hopping, which is excluded for ferromagnetic spin-chains. By Nagaoka's theorem [35], a single hole is expected to turn the system into a ferromagnetic state, in agreement with results for  $\text{La}_5\text{Ca}_9\text{Cu}_{24}\text{O}_{41}$ . However, the experimental observation of antiferromagnetic spin-chains in undoped  $\text{La}_6\text{Ca}_8\text{Cu}_{24}\text{O}_{41}$  is missing so far.

### Acknowledgments

We gratefully acknowledge various fruitful discussions with V. Eyert and T. Kopp, as well as financial support by the Deutsche Forschungsgemeinschaft (SFB 484).

- 
- [1] M. Vojta, Y. Zhang, and S. Sachdev, *Phys. Rev. B* **62**, 6721 (2000).
- [2] T.S. Nunner, P. Brune, T. Kopp, M. Windt, and M. Grüninger, *Phys. Rev. B* **66**, 180404(R) (2002).
- [3] E. Jeckelmann, D.J. Scalapino, and S.R. White, *Phys. Rev. B* **58**, 9492 (1998).
- [4] S. Nishimoto, E. Jeckelmann, and D.J. Scalapino, *Phys. Rev. B* **66**, 245109 (2002).
- [5] N. Motoyama, H. Eisaki, and S. Uchida, *Phys. Rev. Lett.* **76**, 3212 (1996).
- [6] S. Eggert, I. Affleck, and M. Takahashi, *Phys. Rev. Lett.* **73**, 332 (1994).
- [7] S. Eggert, I. Affleck, and M.D.P. Horton, *Phys. Rev. Lett.* **89**, 47202 (2002).
- [8] Y. Mizuno, T. Tohyama, S. Maekawa, T. Osafune, N. Motoyama, H. Eisaki, and S. Uchida, *Phys. Rev. B* **57**, 5326 (1998).
- [9] S. Tornow, O. Entin-Wohlman, and A. Aharony, *Phys. Rev. B* **60**, 10 206 (1999).
- [10] S.L. Drechsler, O. Volkova, A. N. Vasiliev, N. Tristan, J. Richter, M. Schmitt, H. Rosner, J. Malek, R. Klingeler, A.A. Zvyagin, and B. Büchner, *Phys. Rev. Lett.* **98**, 77202 (2007).
- [11] K. Ukei, T. Shishido, and T. Fukuda, *Acta Cryst. B* **50**, 42 (1994).
- [12] Y. Gotoh, I. Yamaguchi, Y. Takahashi, J. Akimoto, M. Goto, M. Onoda, H. Fujino, T. Nagata, and J. Akimitsu, *Phys. Rev. B* **68**, 224108 (2003).
- [13] T. Ohta, F. Izumi, M. Onoda, M. Isobe, E. Takayama-Muromachi, and A.W. Hewat, *J. Phys. Soc. Jpn.* **66**, 3107 (1997).
- [14] M. Matsuda, K. Katsumata, T. Osafune, N. Motoyama, H. Eisaki, S. Uchida, T. Yokoo, S.M. Shapiro, G. Shirane, and J.L. Zarestky, *Phys. Rev. B* **56**, 14499 (1997).
- [15] M. Isobe, M. Onoda, T. Ohta, F. Izumi, K. Kimoto, E. Takayama-Muromachi, A.W. Hewat, and K. Ohoyama, *Phys. Rev. B* **62**, 11667 (2000).
- [16] T. Osafune, N. Motoyama, H. Eisaki, and S. Uchida, *Phys. Rev. Lett.* **78**, 1980 (1997).
- [17] N. Nücker, M. Merz, C.A. Kuntscher, S. Gerhold, S. Schuppler, R. Neudert, M.S. Golden, J. Fink, D. Schild, S. Stadler, V. Chakarian, J. Freeland, Y.U. Idzerda, K. Conder, M. Uehara, T. Nagata, J. Goto, J. Akimitsu, N. Motoyama, H. Eisaki, S. Uchida, U. Ammerahl, and A. Revcolevschi, *Phys. Rev. B* **62**, 14384 (2000).
- [18] M. Matsuda and K. Katsumata, *Phys. Rev. B* **53**, 12201 (1996).
- [19] A. Gelle and M.-B. Lepetit, *Phys. Rev. Lett.* **92**, 236402 (2004); *Eur. Phys. J. B* **43**, 29 (2005).
- [20] R. Klingeler, B. Büchner, K.-Y. Choi, V. Kataev, U. Ammerahl, A. Revcolevschi, and J. Schnack, *Phys. Rev. B* **73**, 014426 (2006).
- [21] U. Schwingenschlögl and C. Schuster, *Europhys. Lett.*, submitted.
- [22] T. Nagata, H. Fujino, J. Akimitsu, M. Nishi, K. Kakurai, S. Katano, M. Hiroi, M. Sera, and N. Kobayashi, *J. Phys. Soc. Jpn.* **68**, 2206 (1999).
- [23] H. Gerdes, A. Bosse, D. Mienert, F.J. Litterst, R. Klingeler, B. Büchner, H.-H. Klauss, *J. Magn. Magn. Mat.* **290-291**, 338 (2005).
- [24] S.A. Carter, B. Batlogg, R.J. Cava, J.J. Krajewski, W.F. Peck Jr., and T.M. Rice, *Phys. Rev. Lett.* **77**, 1378 (1996).
- [25] M. Matsuda, K. Katsumata, T. Yokoo, S.M. Shapiro, and G. Shirane, *Phys. Rev. B* **54**, R15626 (1996).
- [26] R. Leidl and W. Selke, *Phys. Rev. B* **70**, 174425 (2004); R. Leidl, R. Klingeler, B. Büchner, M. Holtschneider, and W. Selke, *Phys. Rev. B* **73**, 224415 (2006).
- [27] C. Schuster and U. Schwingenschlögl, *Phys. Rev. B* **75**, 045124 (2007).

- [28] U. Schwingenschlögl and C. Schuster, *Europhys. Lett.* **79**, 27003 (2007).
- [29] P. Blaha, K. Schwarz, G. Madsen, D. Kvasicka, and J. Luitz, WIEN2k, An Augmented Plane Wave and Local Orbitals Program for Calculating Crystal Properties (TU Wien, Austria, 2001).
- [30] U. Schwingenschlögl, *Phys. Rev. B* **75**, 212408 (2007).
- [31] V. Eyert, U. Schwingenschlögl, and U. Eckern, *Europhys. Lett.* **70**, 782 (2005); *Chem. Phys. Lett.* **390**, 151 (2004).
- [32] U. Schwingenschlögl and V. Eyert, *Ann. Phys. (Leipzig)* **13**, 475 (2004).
- [33] U. Schwingenschlögl and C. Schuster, *Eur. Phys. J. B* **55**, 43 (2007).
- [34] J. Schnack, *Eur. Phys. J. B* **45**, 311 (2005).
- [35] Y. Nagaoka, *Phys. Rev.* **147**, 392 (1966).